Materials International
Open-Access Journal (ISSN: 2668-5728)

Article
Volume 7, Issue 3, 2025, 28
https://doi.org/10.33263/Materials73.028

Development of HPMC/PVA-Based Biodegradable Plastic Derived from the Mucilage of Basil Seeds

N Sandhya Rani [1,*], Shruthi S [2], Madhusudhana R [3]

[1] Department of Applied Physics, Vidyavardhaka College of Engineering, Mysuru, 570-002, India; sandhya.phy@vvce.ac.in;
[2] Department of Chemistry, Mysuru Royal Institute of Technology, Mandya; dr.shruthis@mysururoyal.org;
[3] Department of Physics, ATME College of Engineering, Mysuru – 570028, India; madhusudhanar.phy@atme.edu.in;
* Correspondence: sandhya.phy@vvce.ac.in;

Received: 9.01.2025; Accepted: 25.07.2025; Published: 10.09.2025

Abstract: This study reports the synthesis and characterization of biodegradable plastic films by incorporating basil seed mucilage at two concentrations (5 wt% and 10 wt%) into a hydroxypropyl methylcellulose (HPMC)/polyvinyl alcohol (PVA) polymer matrix. Scanning electron microscopy (SEM) confirmed uniform morphology and surface integrity of the blended films. X-ray diffraction (XRD) analysis showed increased crystallinity at 5 wt% mucilage, followed by a decrease at 10 wt%, suggesting an optimal concentration for structural enhancement. Fourier-transform infrared spectroscopy (FTIR) revealed characteristic vibrational shifts indicating molecular interactions between the mucilage and polymer chains. Mechanical testing demonstrated that films with 5 wt% mucilage exhibited superior tensile strength of 30.66 MPa and tensile modulus of 0.982 GPa compared to the neat blend and 10 wt% counterpart. Biodegradability was assessed via soil burial tests in both dry and moist clay soils, showing up to 40% weight loss in 30 days under moist conditions, indicating significantly accelerated degradation compared to dry soil. These findings highlight the potential of 5 wt.% basil seed mucilage-incorporated HPMC/PVA films as a viable alternative for sustainable bioplastic applications.

Keywords: mucilage of seeds; biodegradation; XRD; mechanical strength.

1. Introduction

A significant portion of environmental plastic waste comprises traditional, non-biodegradable plastics, which pose severe risks to terrestrial and marine life through ingestion or entanglement. In response, biodegradable and compostable alternatives have emerged, designed to decompose in composting facilities and produce safe byproducts for soil and agriculture [1–5]. Biodegradable plastics fully degrade through microbial activity, leaving no toxic residues, making them environmentally preferable. Consequently, many countries have banned conventional plastic bags in favor of biodegradable and compostable options.

Hydroxypropyl methylcellulose (HPMC) and polyvinyl alcohol (PVA) are odorless, tasteless, translucent, water-soluble, non-toxic, semicrystalline, biocompatible, and biodegradable polymers [6–12]. Their blends are widely used as edible, biodegradable films for food packaging and incorporation into food products, combining good mechanical properties with water solubility at ambient temperatures.

Basil (Ocimum spp.), widely cultivated in tropical regions across Asia, Africa, and the Americas, produces seeds that release a white gelatinous mucilage upon hydration [13-14]. Basil seed mucilage (BSM) is a natural polymer comprising proteins, polysaccharides, and uronic acids, accounting for 21–29% of the seed content. It primarily consists of carbohydrates (60.8%), lipids (13.8%), crude protein (13.7%), crude fiber (10.5%), ash (9.5%), and moisture (4.9%), with carbohydrate fractions including cellulose, hemicellulose, and lignin [15 – 19]. BSM is widely utilized as a stabilizing and suspending agent in various applications [20 - 26].

This study investigates the incorporation of varying ratios of BSM (5 wt% and 10 wt%) into HPMC/PVA polymer blends to enhance hydrophilicity, control biodegradation rates, and improve elasticity. These specific concentrations were selected based on preliminary trials aimed at balancing mechanical strength and biodegradability. 5 wt% was expected to enhance tensile properties without compromising film integrity, while 10 wt% was chosen to explore the effects of higher mucilage content on flexibility and degradation rate. Characterizations, including Fourier transform infrared spectroscopy (FTIR), X-ray diffraction (XRD), and scanning electron microscopy (SEM), were performed to analyze functional groups, crystallinity, and morphology. Mechanical tests evaluated tensile strength, and biodegradation assessments examined environmental degradation performance. The results demonstrate that HPMC/PVA films with added BSM form biodegradable thin films suitable for food packaging, carry bags, and related applications.

2. Materials and Methods

2.1. Materials and synthesis of biodegradable thin films.

Basil seeds (Figure 1a) are immersed in distilled water (Figure 1b), which facilitates the release of mucilage contained within the seeds. These soaked seeds are kept at room temperature for 2 to 3 hours. Upon heating to approximately 50°C, the mucilage forms a gel that rises to the surface of the water, while the seeds settle at the bottom of the container. During this heating process, the mixture is continuously stirred to aid in the separation of the mucilage from the seeds. As a result, the seeds remain at the bottom, and the mucilage gel floats on the surface (Figure 1c). A 5 wt% solution of HPMC and PVA is prepared separately. Subsequently, 5 wt% and 10 wt% of mucilage are incorporated into the polymer blend, which is stirred continuously at approximately 70 °C for 4 to 5 hours. The resulting clear solution is then poured onto a clean, flat glass plate and allowed to dry at room temperature for 5 to 6 days. The thin films formed (Figure 1d and Figure 1e) are finally stored in desiccators for subsequent characterization.

(a) **(b)** **(c)** **(d)** **(e)**

Figure 1. (a) Basis seeds; **(b)** soaked in distilled water; **(c)** mucilage separation upon heating; **(d)** HPMC/PVA - 5 wt% mucilage film; **(e)** HPMC/PVA - 10 wt.% mucilage film.

2.2. Instrumentation.

XRD analysis of the films was carried out using an X-ray source with CuKα radiation (wavelength = 1.5406 Å). The surface morphology of the polymer films was examined using a JEOL 840 scanning electron microscope (SEM) operated at 20 kV with a resolution of 10 nm. Prior to imaging, the samples were gold-coated using a sputter coater at 10 mA current under a vacuum of 10^{-2} torr for 3 minutes. Fourier-transform infrared (FTIR) spectra of the films were recorded using a Thermo Nicolet 6700 spectrometer. Measurements were taken over the wavenumber range of 400–4000 cm^{-1}. Tensile testing was conducted on specimens prepared according to ASTM D-638 Type I standard (165 × 19 × 6 mm), as shown in Figure 5.

3. Results and Discussion

3.1. XRD studies.

XRD is highly effective for evaluating the structural characteristics of a sample, identifying its phases, quantitatively analyzing phase mixtures, and determining the degree of crystallinity. In Figure 2, it is evident that all samples display a semicrystalline peak at 2θ = 19.72°. Additionally, there is a noticeable nucleation of crystalline order, resulting in supplementary Bragg-like reflections at approximately 2θ = 29.68° and 2θ = 47.94° across the other samples. The crystallinity percentage for the sample without mucilage was determined to be 56.28%. This value increases to 60.04% upon the incorporation of 5 wt% mucilage, but subsequently decreases to 55.63% with the addition of 10 wt% mucilage. The crystallinity percentage of high-density polyethylene (HDPE), commonly utilized for juice bottles, is also around 60% [27 – 30]. In comparison, the 5 wt% mucilage sample offers a viable alternative to HDPE for domestic applications.

The percentage of the degree of crystallinity (X_c) was determined from the ratios of the area under the crystalline peak and the respective halos using the method [31,32].

$$X_c = \frac{A_c}{A_c + A_a} X\ 100 \qquad (1)$$

Where A_c and A_a are the areas of crystalline and amorphous (halo) regions, respectively.

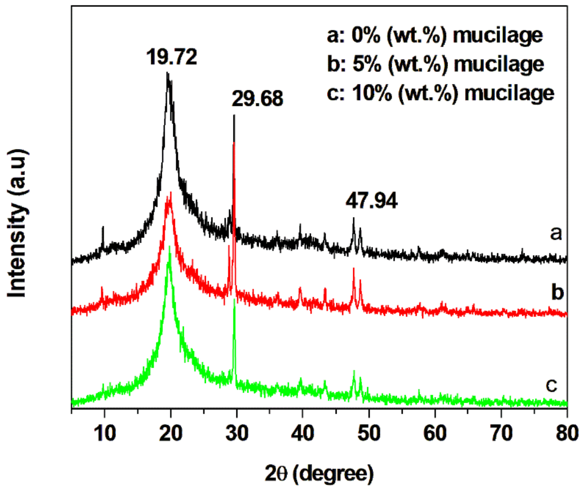

Figure 2. XRD pattern of synthesized biodegradable film samples **(a)** Pure HPMC/PVA; **(b)** HPMC/PVA - 5 wt% mucilage; **(c)** HPMC/PVA - 10 wt% mucilage.

SEM studies.

The SEM micrograph of the Pure HPMC/PVA (0% mucilage) sample reveals a relatively rough and uneven surface with visible micro-voids, which is indicative of poor interfacial compatibility between HPMC and PVA. These discontinuities could potentially serve as crack initiation sites under stress, resulting in moderate mechanical performance. In contrast, the SEM image of the HPMC/PVA-5 wt% mucilage sample shows a significantly smoother and more homogeneous morphology, with fewer surface defects and minimal porosity. This improvement in surface structure implies better dispersion of BSM and enhanced intermolecular interaction with the polymer matrix. The uniform morphology suggests stronger cohesive bonding and reduced phase separation, contributing directly to the enhanced tensile strength and modulus observed in mechanical testing. The reduced porosity in the 5 wt% sample also suggests improved barrier properties and structural integrity, making it more suitable for packaging and load-bearing applications.

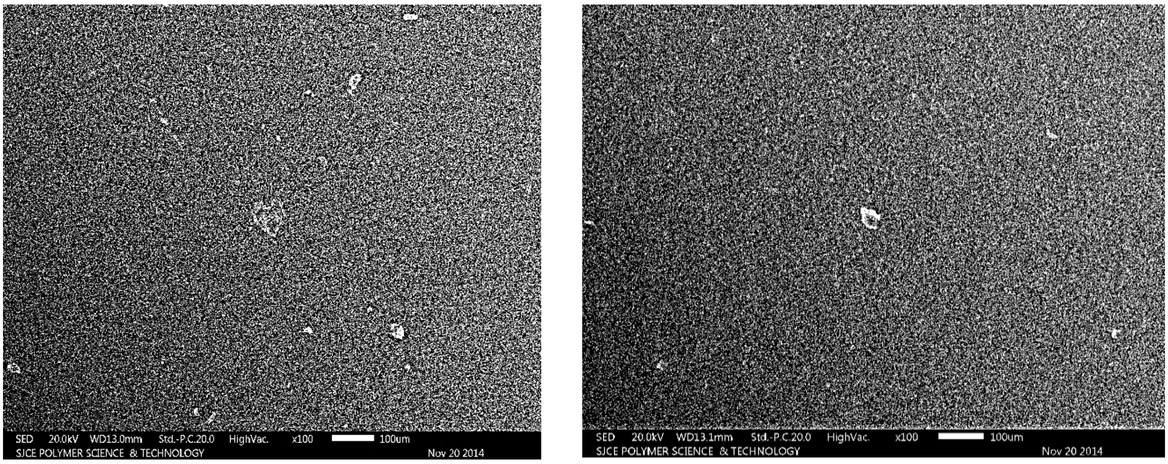

(a) **(b)**

Figure 3. SEM images of **(a)** Pure HPMC/PVA (0% mucilage); **(b)** HPMC/PVA - 5 wt% mucilage.

3.3. FTIR studies.

The FTIR spectra for all samples are presented in Figure 4. The absorption band observed in the range of 3498 cm^{-1} to 3996 cm^{-1} corresponds to the intermolecular hydrogen-bonded O–H stretching vibrations in the polymer–mucilage-based samples. This band shifts to 3496 cm^{-1} to 3585 cm^{-1}, as well as to 3762 cm^{-1} in the 5 wt.% and 10 wt.% mucilage films. The peak at approximately 2928 cm^{-1} corresponds to the aliphatic C–H stretching vibration, associated with the vibrational motion of methyl groups along the polymer chain. Additionally, the peak between 1600 and 1640 cm^{-1} is commonly associated with the presence of water [33,34]. Furthermore, a peak near 1400 cm^{-1} indicates the presence of uronic acid in the polysaccharide derived from basil seed mucilage [35-36]. The peak detected at around 1034 cm^{-1} in all film samples typically corresponds to the asymmetric and symmetric stretching modes of the C–O–C bond within the ether group of the pyranose rings, indicating the presence of monosaccharides. Moreover, the asymmetric bending vibrations of the methyl group in CH_3O at 5 wt.% appear in the absorption range of 1500 cm^{-1} to 1450 cm^{-1}. The absorption peaks observed at 920 cm^{-1} and 850 cm^{-1} correspond to the stretching vibrations of C=C bonds [37]. The analysis revealed that as the concentration of basil mucilage increased, the O–H stretching vibration peaks shifted to higher wavenumbers, while the C–O–C stretching peaks shifted to lower wavenumbers.

In particular, the broad –OH stretching vibration around 3270 cm⁻¹ becomes more intense at 5 wt% mucilage, indicating stronger hydrogen bonding between BSM and the HPMC/PVA matrix. This enhanced bonding correlates with the observed increase in tensile strength (36.69 MPa for 5 wt%, vs. 26.76 MPa for pure HPMC/PVA from Table 1 values). Conversely, at 10 wt.%, a decrease in peak intensity and band broadening suggest reduced intermolecular interactions and phase uniformity, consistent with lower tensile performance (23.19 MPa from Table 1). Additionally, all HPMC/PVA–mucilage films exhibited similar spectral patterns, with no new peaks appearing, indicating that basil seed mucilage is highly compatible with the HPMC/PVA polymer blend matrix. These spectral changes clearly suggest complexation of the seed gel within the polymer matrix.

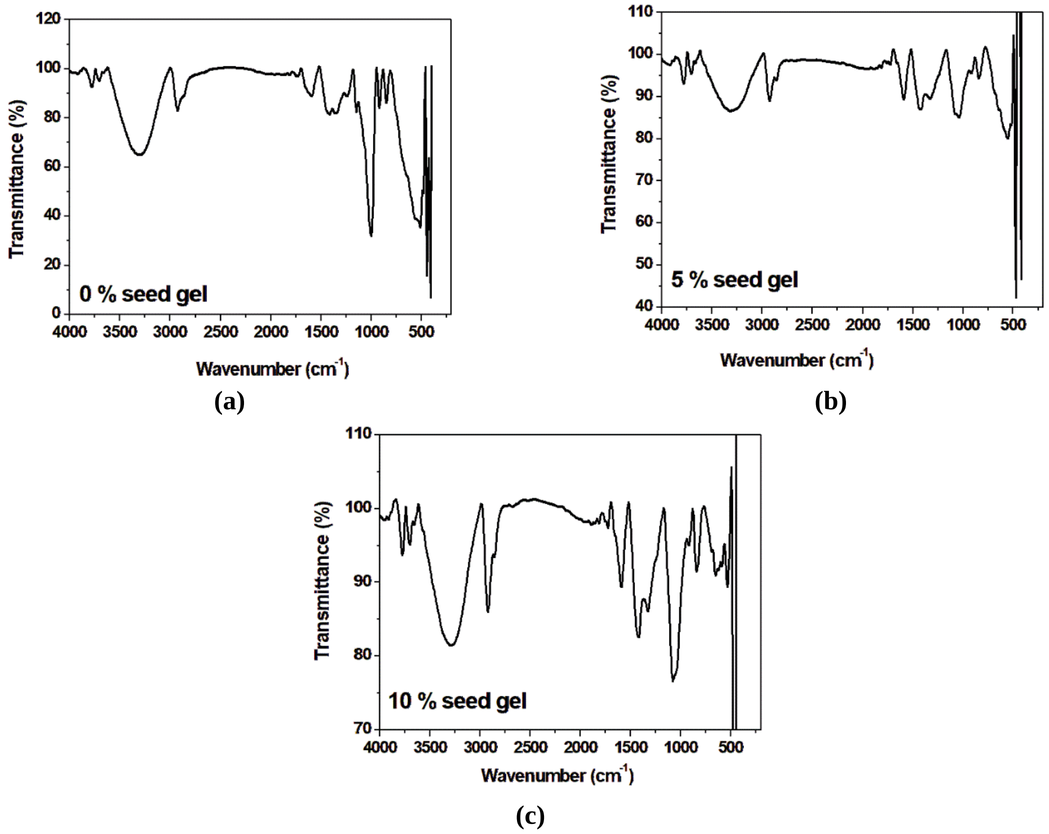

Figure 4. FTIR images of **(a)** Pure HPMC/PVA; **(b)** HPMC/PVA - 5 wt% mucilage; **(c)** HPMC/PVA - 10 wt% mucilage.

3.4. Mechanical property studies.

The load-displacement and stress–strain behavior of the bioplastic samples are illustrated in Figure 6. The neat HPMC/PVA film (0% mucilage) exhibited a tensile strength of 26.76 MPa and a Young's modulus of 0.851 GPa. Incorporation of 5 wt% basil seed mucilage enhanced these values significantly to 36.69 MPa and 0.982 GPa, respectively, indicating improved mechanical strength and stiffness due to better interfacial interaction within the polymer matrix. However, further increasing the mucilage content to 10 wt% resulted in a decline in tensile strength (23.19 MPa) and modulus (0.654 GPa), likely due to phase separation or excess moisture retention, weakening the structure.

This trend demonstrates that 5 wt% mucilage provides the optimal loading, with tensile strength approximately 1.58 times higher than that of the 10 wt% counterpart (Table 1). The yield strength and peak load values further corroborate the superior load-bearing capability at this composition. Notably, the tensile strength of the 5 wt% mucilage film is comparable to that of HDPE (~36 MPa), suggesting its feasibility as a sustainable alternative for high-strength bioplastic applications [38-39].

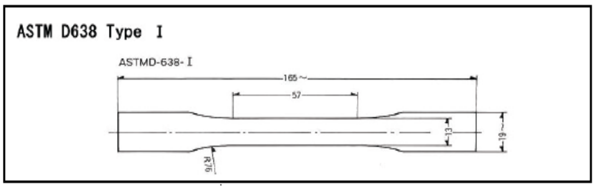

Figure 5. Test specimen for Tensile test (ASTM D638).

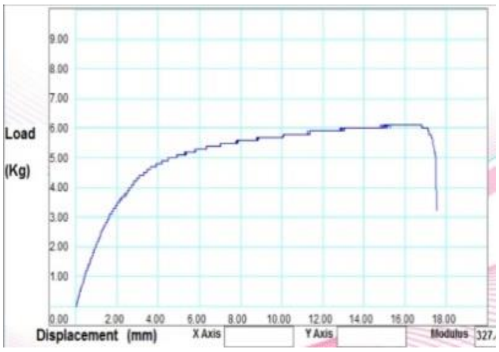

(a)

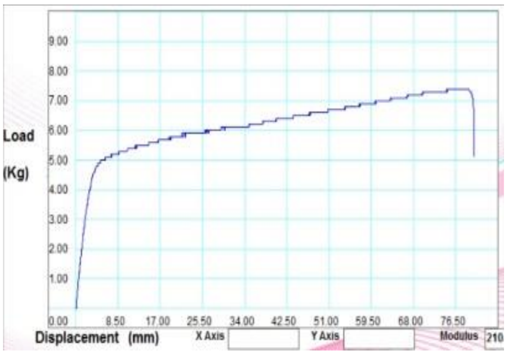

(b)

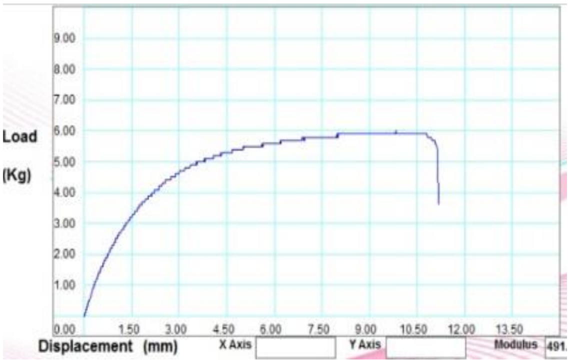

(c)

Figure 6. Load v/s Displacement graph for **(a)** pure HPMC/PVA; **(b)** HPMC/PVA - 5 wt% mucilage; **(c)** HPMC/PVA - 10 wt% mucilage.

Table 1. Tensile strength and modulus.

Sample	Tensile strength (MPa)	Modulus (GPa)	Peak load (kN)	Peak load (kg)
Pure HPMC/PVA (0% mucilage)	26.763	0.851	0.0613	6.1
HPMC/PVA - 5 wt% mucilage	30.661	0.982	0.0768	7.6
HPMC/PVA -10 wt% mucilage	23.192	0.654	0.0578	5.9

3.5. Soil degradation test.

The results regarding biodegradability are crucial for assessing the film's suitability as an environmentally friendly packaging option. Polymers degrade in a bioactive environment through material breakdown, followed by mineralization. Factors such as heat, moisture, and microorganism enzymatic activity contribute to the shortening and weakening of polymer chains. Consequently, the degradation times of films in soil vary depending on the materials used in film production and the surrounding environmental conditions. For instance, Cerruri *et al*. [40] reported a complete dissolution and degradation period of 30 days in their studies involving starch-based polymers. Similarly, Xiong *et al*. [41-42], who also developed starch-based films, reported a degradation time of 100 days.

Samples of 5 wt% basil seed mucilage-added HPMC/PVA polymer film measuring 1 cm × 1 cm were cut and used for the soil degradation experiment (Figures 7a and 7b).

(a) (b) (c) (d)

Figure 7. Cut samples **(a)** and **(b)** to be immersed in **(c)** dry soil; **(d)** clay soil.

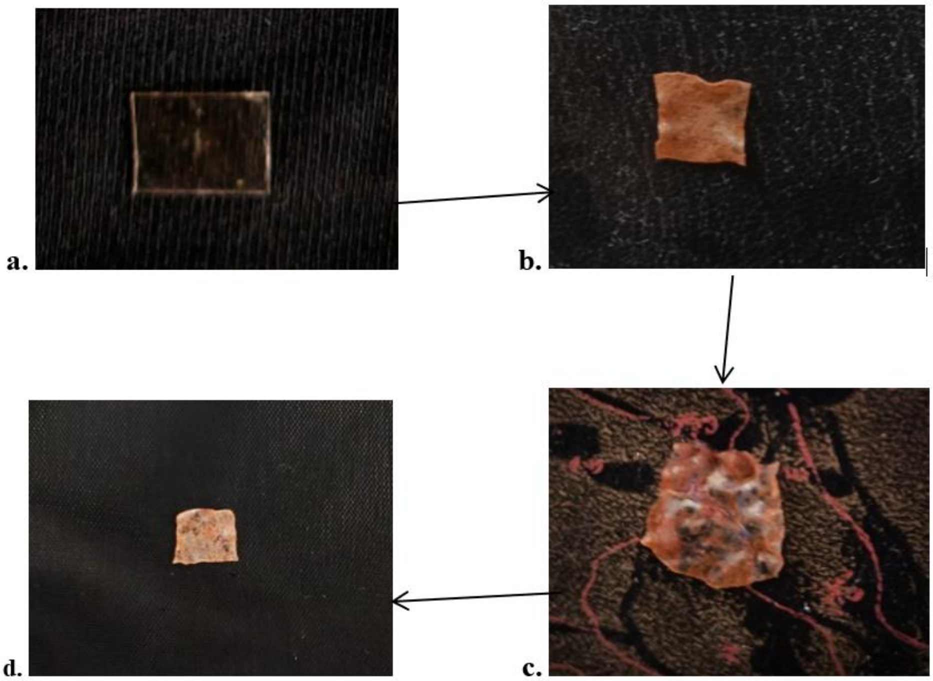

Figure 8. Degradation timeline of HPMC/PVA - 5 wt.% mucilage sample in dry soil: **(a)** Day 1; **(b)** Day 7; **(c)** Day 15; **(d)** Day 20.

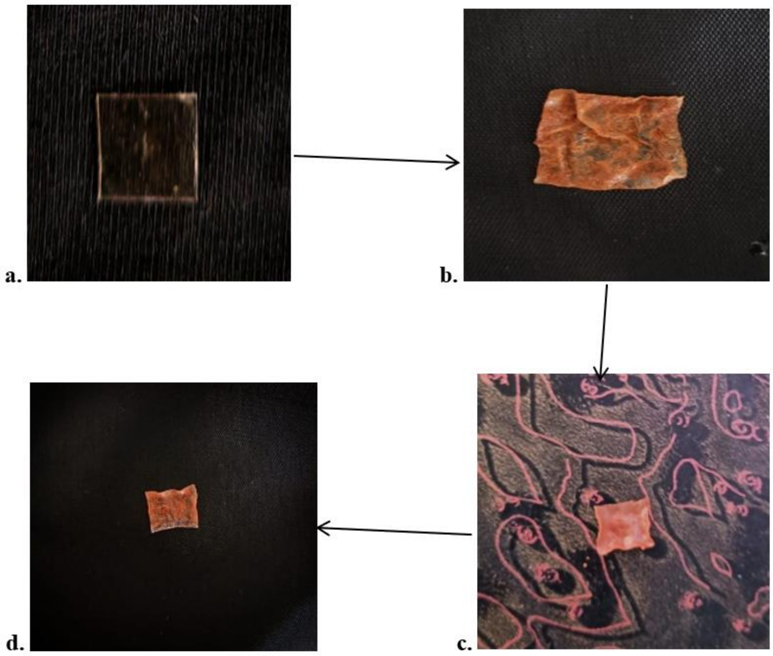

Figure 9. Degradation timeline of HPMC/PVA - 5 wt.% mucilage sample in dry soil: **(a)** Day 1; **(b)** Day 7; **(c)** Day 15; **(d)** Day 20.

These samples were placed in two distinct soil types: dry soil and clay soil, as illustrated in Figures 8c and 8d, respectively. Over time, noticeable deformation in the specimens' shape was observed, indicating mass loss. The samples exhibited shrinkage and disintegration within the first 7 days of soil immersion (Figures 8 and 9). Soil microorganisms play an essential role in the degradation of bioplastics, facilitating the breakdown of biopolymers such as basil mucilage polymer through their enzymatic activity. The reported samples completely disintegrated within 40–45 days.

3.6. Comparative analysis with other bioplastics.

Comparative studies of mechanical properties, degradation times, and crystallinity values for selected bioplastics reported in the literature are depicted in Table 2. To further evaluate the potential of the synthesized HPMC/PVA-based bioplastic films incorporated with basil seed mucilage, a broader comparison with other commonly reported biodegradable polymers is essential. While the mechanical and structural properties were compared with high-density polyethylene (HDPE) in earlier sections, benchmarking against other bio-based polymers helps contextualize the material's practical applicability. Compared to starch- or PCL-based films, the basil seed mucilage–incorporated HPMC/PVA films demonstrate significantly higher tensile strength and better mechanical integrity. While PLA exhibits superior tensile strength, it suffers from slower degradation under ambient conditions and requires industrial composting facilities. In contrast, the synthesized bioplastic here degrades within 40–45 days under natural soil conditions, making it more suitable for single-use packaging and agricultural applications.

The crystallinity of the 5 wt% mucilage sample (60.04%) closely aligns with that of PHBV and chitosan-based films (Table 2), suggesting that the structural ordering in the polymer network supports good barrier and mechanical properties. Moreover, the natural polysaccharide-based mucilage enhances the compatibility and homogeneity of the biopolymer matrix, which is evident from the SEM and FTIR analyses. Thus, in terms of performance metrics—mechanical strength, degradation period, and structural uniformity—the basil seed mucilage-loaded HPMC/PVA films offer a competitive, eco-sustainable alternative to synthetic plastics and a viable option among plant-based bioplastics.

Table 2. Comparative summary of mechanical properties (tensile strength, modulus), degradation time, and crystallinity values from selected bioplastics reported in the literature.

Bioplastic Material	Tensile Strength (MPa)	Young's Modulus (GPa)	Degradation Time	Crystallinity (%)	References
HPMC/PVA + 5% BSM	36.69	0.982	40–45 days	60.04	This study
Starch-based film (without filler)	8–15	0.1–0.4	30–100 days	20–30	[40 - 42]
PLA (Polylactic Acid)	40–60	2.0–3.5	180–250 days	~37–40	[3]
PHBV	22–35	1.5–2.2	60–120 days	55–70	[43]
PCL (Polycaprolactone)	10–20	0.2–0.4	60–90 days	~45	[46]
Chitosan-based bioplastic	25–30	0.8–1.0	35–50 days	~50	[44]
HPMC + Mg salt	28–32	0.85–0.95	~45 days	~58	[45]

3.7. Summary comparison table: bioplastic samples.

The table below summarizes key differences in structural, mechanical, and morphological properties of HPMC/PVA-based bioplastic films with and without basil seed mucilage (BSM). This helps highlight the advantages of incorporating 5 wt% BSM into the polymer matrix.

Table 3. Summary comparison between the HPMC/PVA (0 and 5 wt% mucilage) films.

Property	Pure HPMC/PVA (0 wt% mucilage)	HPMC/PVA – 5 wt% mucilage	Implication
Surface morphology (SEM)	Rough, with voids and cracks	Smooth, dense, fewer voids	Better interfacial bonding and mechanical integrity
Tensile Strength (MPa)	26.76 MPa	36.69 MPa	Improved load-bearing capacity
Modulus (GPa)	0.851 GPa	0.982 GPa	Greater stiffness and resistance to deformation
Crystallinity (XRD)	Moderate	High	Enhanced structural order and packing
FTIR Shift	Baseline functional groups of HPMC/PVA	Shifts in OH and CO peaks	Evidence of interaction between BSM and polymer matrix
Biodegradation Rate	Slower	Faster in moist soil	Accelerated degradation in natural environments

4. Conclusions

A rapidly biodegradable, non-toxic, and environmentally friendly plastic suitable for various applications, such as carry bags and food packaging, has been successfully developed by incorporating 5 wt% basil seed mucilage into an HPMC/PVA polymer matrix. Scanning electron microscopy analysis confirmed the uniform morphological structure of the produced samples. X-ray Diffraction results indicated an increase in crystallinity at 5 wt% mucilage. At the same time, a decrease was observed at 10 wt%, suggesting that the optimal mucilage incorporation ratio in the HPMC/PVA blend is 5 wt%. Fourier transform infrared spectroscopy studies demonstrated vibrational changes associated with varying mucilage ratios within the polymer matrix. Mechanical testing revealed that films containing 5 wt% mucilage exhibited enhanced tensile strength and modulus. A soil degradation assessment was conducted to evaluate the biodegradability of the films in both dry and moist clay soils, revealing that they degraded more rapidly in moist clay soil than in dry soil. The synthesized materials present promising options for biodegradable plastic applications. Future studies should focus on scaling up the synthesis process, assessing shelf-life and barrier properties, and evaluating environmental safety under real-world conditions to facilitate commercial application.

Author Contributions

Conceptualization, N.S.R.; methodology, N.S.R.; investigation, N.S.R.; validation, N.S.R.; visualization, N.S.R.; writing—original draft preparation, N.S.R.; formal analysis, S.S. (supporting); data curation, M.R.; software, M.R. (supporting); writing—review and editing, M.R.; supervision, N.S.R. All authors have read and agreed to the published version of the manuscript.

Institutional Review Board Statement

Not applicable.

Informed Consent Statement

Not applicable.

Data Availability Statement

Not applicable.

Funding

This research received no external funding.

Acknowledgments

The authors gratefully acknowledge the management of Vidyavardhaka College of Engineering, Mysuru, for providing financial support for this study. We thank SJCE, Mysuru, for providing XRD, SEM, and FTIR facilities, respectively, for the reported study.

Conflict of Interest

The author declares no conflict of interest.

References

1. Altaee, N.; El-Hiti, G.A.; Fahdil, A.; Sudesh, K.; Yousif, E. Biodegradation of different formulations of polyhydroxybutyrate films in soil. *Springer Plus* **2016**, *5*, 762, https://doi.org/10.1186/s40064-016-2480-2.
2. Arcos-Hernandez, M.V.; Laycock, B.; Pratt, S.; Donose, B.C.; Nikoli´c, M.A.L.; Luckman, P.; Werker, A.; Lant, P.A. Biodegradation in a soil environment of activated sludge derived polyhydroxyalkanoate (PHBV). *Polym. Degrad. Stabil*. **2012**, *97*, 2301-2312, https://doi.org/10.1016/j.polymdegradstab.2012.07.035.
3. Philip, S.; Keshavarz, T.; Roy, I. Review Polyhydroxyalkanoates biodegradable polymers with a range of applications. *J. Chem. Technol. Biotechnol*. **2007**, *82*, 233-47, https://doi.org/10.1002/jctb.1667.
4. Moshood, T.D.; Nawanir, G.; Mahmud, F.; Mohamad, F.; Ahmad, M.H.; AbdulGhani, A. Sustainability of biodegradable plastics: New problem or solution to solve the global plastic pollution?. *Curr. Res. Green Sustain. Chem.* **2022**, *5*, 100273, https://doi.org/10.1016/j.crgsc.2022.100273.
5. Peidayesh, H.; Heydari, A.; Mosnáˇcková, K.; Chodak, I. In situ dual crosslinking strategy to improve the physico-chemical properties of thermoplastic starch. *Carbohydr. Polym*. **2021**, *269*, 118250, https://doi.org/10.1016/j.carbpol.2021.118250.
6. Chowdhury, R.A.; Sadri, A.M.; Hoque, M.E. 18 - Industrial implementations of biocomposites. In Green Biocomposites for Biomedical Engineering, Hoque, M.E., Sharif, A., Jawaid, M., Eds.; Woodhead Publishing: **2021**; pp. 391-408, https://doi.org/10.1016/B978-0-12-821553-1.00020-X.
7. Rotta, J.; Minatti, E.; Barret, P.L.M. Determination of structural and mechanical properties, diffractometry, and thermal analysis of chitosan and hydroxypropylmethylcellulose (HPMC) films plasticized with sorbitol. *Food Sci. Technol.* **2011**, *31*, 450–455, https://doi.org/10.1590/S0101-20612011000200026.
8. Kanakaraj, T.M.; Bhajantri, R.F.; Chavan, C.; Cyriac, V.; Bulla, S.S.; Ismayil. Investigation on the structural and ion transport properties of magnesium salt doped HPMC-PVA based polymer blend for energy storage applications. *J. Non-Cryst. Solids* **2023**, *609*, 122276, https://doi.org/10.1016/j.jnoncrysol.2023.122276.
9. Sandhya Rani, N.; Sannappa, J.; Demappa, T.; Mahadevaiah. structural, thermal, and electrical studies of sodium iodide (NaI)-doped hydroxypropyl methylcellulose (HPMC) polymer electrolyte films. *Ionics* **2014**, *20*, 201-207, https://doi.org/10.1007/s11581-013-0952-8.
10. Sandhya Rani, N.; Sannappa, J.; Demappa, T.; Mahadevaiah. Effects of CdCl2 concentration on the structural, thermal and ionic conductivity properties of HPMC polymer electrolyte films. *Ionics* **2015**, *21*, 133–140, https://doi.org/10.1007/s11581-014-1151-y.
11. Nouh, S.A.; Abdel-Kader, M.H.; Mohamed, M.B. Structural and optical modifications in polyvinyl alcohol due to Cr_2O_3 nanoparticles additives concentration, and gamma irradiation. *Adv. Polym. Technol.* **2017**, *36*, 336-340, https://doi.org/10.1002/adv.21614.
12. Senthil, R.; Wilson Aruni, A.; Turkmen, H. Eco-friendly bioenergy: New approaches for the effective treatment of tannery fleshings. *Environ. Chall.* **2021**, *5*, 100249, https://doi.org/10.1016/j.envc.2021.100249.
13. Nigam, S.; Das, A.K.; Patidar, M.K. Synthesis, characterization and biodegradation of bioplastic films produced from Parthenium hysterophorus by incorporating a plasticizer (PEG600). *Environ. Chall.* **2021**, *5*, 100280, https://doi.org/10.1016/j.envc.2021.100280.
14. Tanavar, H.; Barzegar, H.; Alizadeh Behbahani, B.; Mehrnia, M.A. Investigation of the chemical properties of Mentha pulegium essential oil and its application in Ocimum basilicum seed mucilage edible coating for

extending the quality and shelf life of veal stored in refrigerator (4°C). *Food Sci. Nutr.* **2021**, *9*, 5600-5615, https://doi.org/10.1002/fsn3.2522.

15. Anand, S.; Mahajan, D.; Kataki, S.; Chatterjee, S.; Sharma, P.K.; Rai, P.K.; Narang, R. Conceptualizing a novel Hybrid Decontamination System (HDS) based on UV/H2O2 treatment for the enhanced decontamination and reuse of N95 FFRs. *Environ. Chall.* **2021**, *5*, 100276, https://doi.org/10.1016/j.envc.2021.100276.
16. Ani, K.A.; Agu, C.M.; Menkiti, M.C. Preliminary investigation and neural network modeling of palm oil mill effluent as a potential bio-stimulating organic co-substrate in hydrocarbon degradation. *Environ. Chall.* **2021**, *5*, 100216, https://doi.org/10.1016/j.envc.2021.100216.
17. Noshad, M.; Alizadeh Behbahani, B.; Jooyandeh, H.; Rahmati-Joneidabad, M.; Hemmati Kaykha, M.E.; Ghodsi Sheikhjan, M. Utilization of Plantago major seed mucilage containing Citrus limon essential oil as an edible coating to improve shelf-life of buffalo meat under refrigeration conditions. *Food Sci. Nutr.* **2021**, *9*, 1625-1639, https://doi.org/10.1002/fsn3.2137.
18. Ali, M.R.; Parmar, A.; Niedbała, G.; Wojciechowski, T.; Abou El-Yazied, A.; El-Gawad, H.G.A.; Nahhas, N.E.; Ibrahim, M.F.M.; El-Mogy, M.M. Improved Shelf-Life and Consumer Acceptance of Fresh-Cut and Fried Potato Strips by an Edible Coating of Garden Cress Seed Mucilage. *Foods* **2021**, *10*, 1536, https://doi.org/10.3390/foods10071536.
19. Sabahi, S.; Abbasi, A.; Mortazavi, S.A. Characterization of cinnamon essential oil and its application in Malva sylvestris seed mucilage edible coating to the enhancement of the microbiological, physicochemical and sensory properties of lamb meat during storage. *J. Appl. Microbiol.* **2022**, *133*, 488-502, https://doi.org/10.1111/jam.15578.
20. Siko, I.; Sola, P.; Mulwa, R.; Otieno, P. Evaluating charcoal producers' preferences for improved production systems in Marigat sub county, Baringo County. *Environ. Chall.* **2021**, *5*, 100275, https://doi.org/10.1016/j.envc.2021.100275.
21. Tosif, M.M.; Najda, A.; Bains, A.; Zawiślak, G.; Maj, G.; Chawla, P. Starch–mucilage composite films: An inclusive on physicochemical and biological perspective. *Polymers* **2021**, *13*, 2588, https://doi.org/10.3390/polym13162588.
22. Mannai, F.; Mechi, L.; Alimi, F.; Alsukaibi, A.K.D.; Belgacem, M.N. Biodegradable composite films based on mucilage from Opuntia ficus-indica (Cactaceae): Microstructural, functional and thermal properties. *Int. J. Biol. Macromol.* **2023**, *252*, 126456, https://doi.org/10.1016/j.ijbiomac.2023.126456.
23. Li, X.; Ren, Z.; Wang, R.; Liu, L.; Zhang, J.; Ma, F.; Khan, M.Z.H.; Zhao, D.; Liu, X. Characterization and antibacterial activity of edible films based on carboxymethyl cellulose, Dioscorea opposita mucilage, glycerol and ZnO nanoparticles. *Food Chem.* **2021**, *349*, 129208, https://doi.org/10.1016/j.foodchem.2021.129208.
24. Davoudi, S.; Zandi, M.; Ganjloo, A. Fabrication and characterization of novel biodegradable films based on tomato seed mucilage and gelatin plasticized with polyol mixtures. *Food Bioprod. Process* **2024**, *148*, 187-197, https://doi.org/10.1016/j.fbp.2024.09.015.
25. Aaliya, B.; Sunooj, K.V.; Vijayakumar, A.; Krina, P.; Navaf, M.; Akhila, P.P.; Raviteja, P.; Mounir, S.; Lackner, M.; George, J. Fabrication and characterization of talipot starch-based biocomposite film using mucilages from different plant sources: A comparative study. *Food Chem.* **2024**, *438*, 138011, https://doi.org/10.1016/j.foodchem.2023.138011.
26. Urbizo-Reyes, U.; San Martin-González, M.F.; Garcia-Bravo, J.; Liceaga, A.M. Development of chia seed (Salvia hispanica) mucilage films plasticized with polyol mixtures: Mechanical and barrier properties. *Int. J. Biol. Macromol.* **2020**, *163*, 854-64, https://doi.org/10.1016/j.ijbiomac.2020.07.023.
27. Shiam, M.A.; Islam, M.S.; Ahmad, I.; Haque, S.S. A review of plant-derived gums and mucilages: Structural chemistry, film forming properties and application. *J. Plastic Film Sheeting* **2025**, *27*, 87560879251316553, https://doi.org/10.1177/87560879251316553.
28. Van Rooyen, B.; De Wit, M.; Osthoff, G.; Van Niekerk, J.; Hugo, A. Effect of Native Mucilage on the Mechanical Properties of Pectin-Based and Alginate-Based Polymeric Films. *Coatings* **2023**, *13*, 1611, https://doi.org/10.3390/coatings13091611.
29. Scognamiglio, F.; Gattia, D.M.; Roselli, G.; Persia, F.; De Angelis, U.; Santulli, C. Thermoplastic Starch (TPS) films added with mucilage from Opuntia Ficus Indica: Mechanical, microstructural and thermal characterization. *Materials* **2020**, *13*, 1000, https://doi.org/10.3390/ma13041000.
30. Davachi, S.M.; Pottackal, N.; Torabi, H. Development and characterization of probiotic mucilage based edible films for the preservation of fruits and vegetables. *Sci. Rep.* **2021**, *11*, 16608, https://doi.org/10.1038/s41598-021-95994-5.

31. Alzerreca, M.; Paris, M.; Boyron, O.; Orditz, D.; Louarn, G.; Correc, O. Mechanical properties and molecular structures of virgin and recycled HDPE polymers used in gravity sewer systems. *Polym. Test* **2015**, *46*, 1-8, https://doi.org/10.1016/j.polymertesting.2015.06.012.
32. Ghadiri Alamdari, N.; Salmasi, S.; Almasi, H. Tomato Seed Mucilage as a New Source of Biodegradable Film-Forming Material: Effect of Glycerol and Cellulose Nanofibers on the Characteristics of Resultant Films. *J. Food Bioprocess Technol.* **2021**, *14*, 2380–2400, https://doi.org/10.1007/s11947-021-02734-8.
33. Smaoui, S.; Chérif, I.; Ben Hlima, H.; Khan, M.U.; Rebezov, M.; Thiruvengadam, M.; Sarkar, T.; Shariati, M.A.; Lorenzo, J.M. Zinc oxide nanoparticles in meat packaging: A systematic review of recent literature. *Food Packag. Shelf Life* **2023**, 36, 101045, https://doi.org/10.1016/j.fpsl.2023.101045.
34. Kurt, A.; Kahyaoglu, T. Characterization of a new biodegradable edible film made from salep glucomannan. *Carbohydr. Polym.* **2014**, *104*, 50–58, https://doi.org/10.1016/j.carbpol.2014.01.003.
35. Naji-Tabasi, S.; Razavi, S.M.A.; Mohebbi, M.; Malaekeh-Nikouei, B. New studies on basil (Ocimum bacilicum L.) seed gum: Part I - Fractionation, physicochemical and surface activity characterization. *Food Hydrocoll.* **2016**, *52*, 350–358, https://doi.org/10.1016/j.foodhyd.2015.07.011.
36. Hashemi Gahruie, H.; Mostaghimi, M.; Ghiasi, F. The effects of fatty acids chain length on the technofunctional properties of basil seed gum-based edible films. *Int. J. Biol. Macromol.* **2020**, *160*, 245, https://doi.org/10.1016/j.ijbiomac.2020.05.136.
37. Thessrimuang, N.; Prachayawarakorn, J. Development, modification and characterization of new biodegradable film from basil seed (Ocimum basilicum L.) mucilage. *J. Sci. Food Agric*. **2019**, *99*, 5508–5515, https://doi.org/10.1002/jsfa.9812.
38. Pelto, J.; Verho, T.; Ronkainen, H.; Kaunisto, K.; Metsäjoki, J.; Seitsonen, J. Matrix morphology and the particle dispersion in HDPE nanocomposites with enhanced wear resistance. *Polym Test* **2019**, *77*, 105897, https://doi.org/10.1016/j.polymertesting.2019.105897.
39. Woggum, T.; Sirivongpaisal, P.; Wittaya, T. Properties and characteristics of dual-modified rice starch-based biodegradable films. *Int. J. Biol. Macromol.* 2014, 67, 490–502, https://doi.org/10.1016/j.ijbiomac.2014.03.029.
40. Peidayesh, H.; Mosnáčková, K.; Špitalský, Z.; Heydari, A.; Šišková, A.O.; Chodák, I. Thermoplastic starch–based composite reinforced by conductive filler networks: Physical properties and electrical conductivity changes during cyclic deformation. *Polymers* **2021**, *13*, 3819, https://doi.org/10.3390/polym13213819.
41. Amaraweera, S.M.; Gunathilake, C.; Gunawardene, O.H.; Fernando, N.M.; Wanninayaka, D.B.; Dassanayake, R.S.; Rajapaksha, S.M.; Manamperi, A.; Fernando, C.A.; Kulatunga, A.K. Development of starch-based materials using current modification techniques and their applications: A review. *Molecules* **2021**, *26*, 6880, https://doi.org/10.3390/molecules26226880.
42. Cerruti, P.; Santagata, G.; d'Ayala, G.G.; Ambrogi, V.; Carfagna, C.; Malinconico, M.; Persico, P. Effect of a natural polyphenolic extract on the properties of a biodegradable starch-based polymer. *Polym. Degrad. Stab.* **2011**, *96*, 839-846, https://doi.org/10.1016/J.polymergradstab.2011.02.003.
43. Sudesh, K.; Abe, H.; Doi, Y**.** Synthesis, structure and properties of polyhydroxyalkanoates: Biological polyesters. *Prog. Polym. Sci***. 2000**, 25, 1503–1555, https://doi.org/10.1016/S0079-6700(00)00035-6.
44. Espitia, P. J. P.; Du, W.-X.; de Jesús Avena-Bustillos, R.; Soares, N. de F. F.; McHugh, T. H. Edible films from pectin incorporating zinc oxide nanoparticles: A new strategy for extending food shelf life. *Food Hydrocolloids* **2014**, 35, 287–296. https://doi.org/10.1016/j.foodhyd.2013.06.005.
45. Du, J.; Zhu, Q.; Guo, J.; Gu, J.; Guo, J.; Wu, Y.; Ren, L.; Yang, S.; Jiang, J. Preparation and characterization of edible films from gelatin and hydroxypropyl methyl cellulose/sodium carboxymethyl cellulose. Heliyon **2025**, 11(1), e41613, https://doi.org/10.1016/j.heliyon.2024.e41613.
46. Wei, X.; Gong, C.; Gou, M.; Fu, S.; Guo, Q.; Shi, S.; Luo, F.; Guo, G.; Qiu, L.; Qian, Z**.** Biodegradable poly(ε-caprolactone)–poly(ethylene glycol) copolymers as drug delivery system. Int. J. Pharm. **2009**, 381(1), 1–18, https://doi.org/10.1016/j.ijpharm.2009.07.033.

Publisher's Note & Disclaimer